



**HAL**  
open science

## Very slow creep tests on rock samples

Pierre Bérest, Pierre Antoine Blum, Jean Pierre Charpentier, Hakim Gharbi,  
Frédéric Valès

► **To cite this version:**

Pierre Bérest, Pierre Antoine Blum, Jean Pierre Charpentier, Hakim Gharbi, Frédéric Valès. Very slow creep tests on rock samples. *International Journal of Rock Mechanics and Mining Sciences*, 2005, 42 (4), pp.569-576. 10.1016/j.ijrmms.2005.02.003 . hal-00111443

**HAL Id: hal-00111443**

**<https://hal.science/hal-00111443>**

Submitted on 20 Apr 2024

**HAL** is a multi-disciplinary open access archive for the deposit and dissemination of scientific research documents, whether they are published or not. The documents may come from teaching and research institutions in France or abroad, or from public or private research centers.

L'archive ouverte pluridisciplinaire **HAL**, est destinée au dépôt et à la diffusion de documents scientifiques de niveau recherche, publiés ou non, émanant des établissements d'enseignement et de recherche français ou étrangers, des laboratoires publics ou privés.



Distributed under a Creative Commons Attribution - NonCommercial 4.0 International License

# Very slow creep tests on rock samples

Pierre Bérest<sup>a,\*</sup>, Pierre Antoine Blum<sup>b</sup>, Jean Pierre Charpentier<sup>a</sup>, Hakim Gharbi<sup>a</sup>,  
Frédéric Valès<sup>a</sup>

<sup>a</sup>Laboratoire de Mécanique des Solides, Ecole polytechnique, Palaiseau cedex 91128, France

<sup>b</sup>Institut de Physique du Globe de Paris, Jussieu, 75005 Paris, France

## 1. Introduction

For the past several years, there has been growing concern about the long-term behaviour of deep underground openings. Immediately after a deep (500–1500 m) cavern or gallery is opened in a soft rock (rock salt, marls, argillite), the rock mass experiences relatively large viscoplastic strain rates. However, after a couple of years, the strain rates become smaller and reach a more-or-less steady state characterized by very small strain rates. Brouard [1] performed an in-situ measurement of a 1000-m deep, 12-yr-old brine-filled salt cavern and proved that the steady-state cavern volume loss rate was  $\dot{V}/V = -3 \times 10^{-4} \text{ yr}^{-1}$  (i.e.,  $10^{-11} \text{ s}^{-1}$ ). Such a rate is typical of salt caverns at this depth and can be disregarded when short-term operation is concerned. However, with regard to the behaviour of a closed and abandoned cavern, this rate governs the build-up rate of brine pressure [2].

Moreover, when smaller periods of time are considered, the stress distribution around a cavern or a gallery is such that the deviatoric stress rapidly decreases with respect to the distance to the cavern. Very small strain rates are experienced at large distances inside the rock mass, and they must be assessed when predicting cavern or gallery behaviour.

In other words, when computing the behaviour of such openings, the mechanical behaviour of the rock is of interest in the strain-rate range of  $\dot{\epsilon} = 10^{-14} - 10^{-11} \text{ s}^{-1}$ .

Such small rates have not been widely investigated in the literature, despite their role with regard to geological deformations. The behaviour of rock salt, which essentially is a viscoplastic rock, has been studied extensively in the strain-rate range  $\dot{\epsilon} = 10^{-10} - 10^{-6} \text{ s}^{-1}$  (see [3–7]). Hunsche [8] describes the measurement of creep in rock salt at small strain rates using a special testing device; the test lasted approximately 1 week;  $\dot{\epsilon} = 7 \times 10^{-12} \text{ s}^{-1}$  was “the lowest reliably determined deformation rate” [8, p. 194].

The limited available literature is probably inherent to the particular problems raised by long-term, small-rate creep tests, as noted below

1. When the creep rate is  $\dot{\epsilon} = 10^{-12} \text{ s}^{-1}$ , a test lasting 12 days results in a strain of  $\epsilon = 10^{-6}$ . The thermal expansion coefficient of rocks is of the order  $\alpha = 1 - 4 \times 10^{-5} \text{ }^\circ\text{C}^{-1}$ —that is, the “noise” (i.e., sample thermo-elastic deformation) due to small temperature variations will be larger, in most cases, than the signal to be measured (i.e., sample average deformation originated by creep proper). The same can be said of hygrometric variations, whose influence is large for many rocks [9,10].
2. Slow creep rates are obtained when small mechanical loadings are applied. Most creep test devices are designed to operate in the deviatoric stress range of 5–20 MPa. Stress control is usually poor when the applied stress is smaller than 1 MPa.
3. Creep rate is computed by comparing the strains  $\epsilon_1, \epsilon_2$  measured at two different times,  $t_1$  and  $t_2$ , or  $\dot{\epsilon} = (\epsilon_2 - \epsilon_1)/(t_2 - t_1)$ . When the strain rate is in the range  $\dot{\epsilon} = 10^{-12} \text{ s}^{-1}$ , it can be assessed reasonably on

\*Corresponding author. Tel.: +33 1 69 33 41 28;  
fax: +33 1 69 33 30 28.

E-mail address: berest@lms.polytechnique.fr (P. Bérest).

a daily basis ( $t_2 - t_1 = 10^5$  s,  $\varepsilon_2 - \varepsilon_1 = 10^{-7}$ ) only if  $\varepsilon_1$  and  $\varepsilon_2$  can be measured with an accuracy of at least  $10^{-8}$ , or one-tenth of the expected difference between the two consecutive measured strains.

In other words, accurate long-term creep tests are possible only when there is very accurate measurement of sample length change, when the applied load remains constant, and when the temperature and hygrometry experience very small changes. This note describes such experiments performed in underground rooms (to take advantage of very stable temperature) using an extremely accurate sensor and dead-weight loading.

## 2. Description and discussion of the testing system

### 2.1. Testing device

Long-term uniaxial creep tests were conducted on standard cylindrical rock samples (diameter  $D = 70$  mm, height  $H = 160$  mm). The sample was set between two stiff silica plates (Fig. 1), with a steel cap set between the sample and the upper silica plate. During each test, four high-resolution displacement sensors set in two vertical planes at a  $90^\circ$  angle allowed both the relative rotation of the two plates and their average relative displacement to be measured.

### 2.2. Sensors

The sensors [Fig. 2(a)] were designed by P.A. Blum, of the Institut de Physique du Globe de Paris [11]. A vertical silica rod is fixed to the upper plate; at its lower tip, a silica drop encapsulates a ferritic element that moves up and down inside a vertical silica tube that bears a magnetic coil and is fixed to the lower plate. Silica is used to minimize the effects of thermal perturbations. Small displacements of the ferritic element generate voltage, which is recorded. A  $1\text{-}\mu\text{m}$  displacement generates a  $1\text{-mV}$  voltage. Because  $1\text{-}\mu\text{V}$  tension can be measured easily, measurement of a  $10^{-8}$

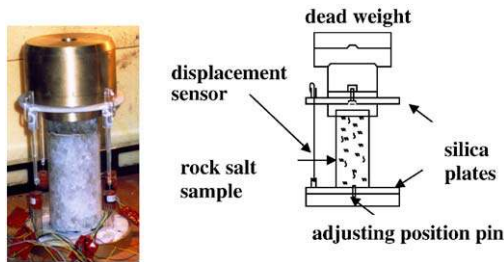


Fig. 1. Rock-salt testing device. Samples are 160-mm high. Four displacement sensors were used during each test.

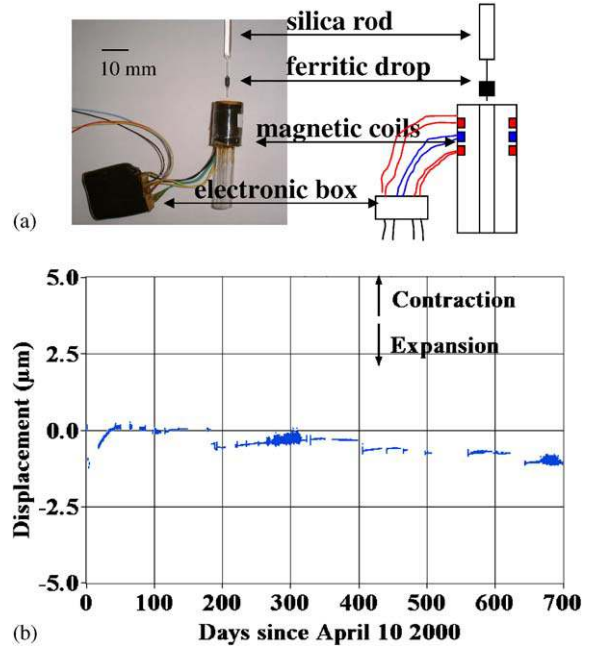


Fig. 2. Displacement sensor details (a) and sensor drift (b).

strain variation on a sample 100-mm high can be expected.

Because tests last several hundred days, sensor drift is a concern. Reference tests were performed and a number of sensors larger than what was strictly necessary were used.

#### 2.2.1. Sensor drift: reference tests

A 2-yr reference test was performed on a 10-cm long sensor in one of the underground testing sites, the La Brasserie Quarry. The upper and lower parts of a reference sensor were fixed to a rigid frame. No movement was expected. The displacement-versus-time curve shows that the sensor drift is  $1\text{-}\mu\text{m}$  after 700 days (or 2 yr), or  $10^{-13}\text{ s}^{-1}$  [Fig. 2(b)].

In the Varangéville salt mine, the second test site, a reference test was performed on a duralumin sample (Varangéville Test no. 0). The sample bore no load except for the upper plate weight; the sample height was 20 cm. No delayed deformation was expected. In fact, the observed mean deformation was only four times smaller than the deformation of the loaded salt samples (see Section 3), casting doubt on the absence of a drift. However, during this specific test, small glue dots had been left between the lower plate and the duralumin sample to make sample setting easier. In hindsight, this proved to be a mistake, as it is suspected that the unexpectedly observed small deformation rate was caused by the crushing of the glue dots rather than by an actual drift. This test was stopped after 1 yr. In the

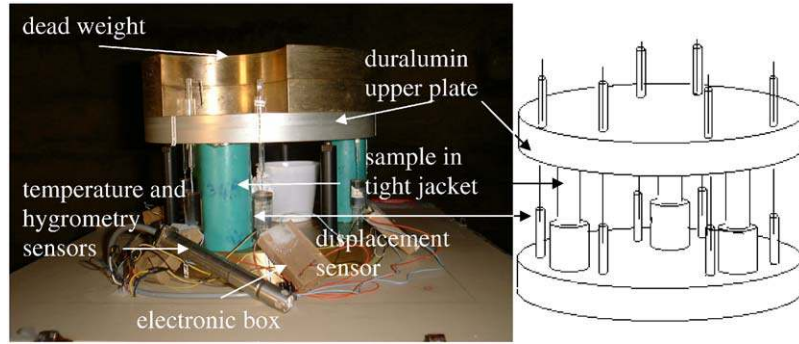


Fig. 3. Argillite creep testing device. Three samples (diameter  $D = 36$  mm, height  $H = 72$  mm) were tested together; six displacement sensors were used.

other tests, an adjusting pin was used instead of glue dots (see Fig. 1).

### 2.2.2. Sensor drift: consistency of the measured displacements

A purely rigid movement (rotation + vertical displacement) of the stiff upper plate can be expected during the tests. To detect such movement, three sensors are needed. During the tests performed on the rock-salt samples in the Varangéville Mine, four sensors were used during each test to provide redundancy. The results provided by the four sensors proved to be consistent (see Section 2.4), providing confidence in sensor behaviour. However during the course of each series of tests, one or two of the four sensors failed, either temporarily or permanently, and no further comparison was possible. Furthermore, indirect proof of the absence of a very large sensor drift lays in the fact that, even when submitted to a relatively complex stress history (Varangéville Test no. 1; see Section 3), a sample exhibits the same general features as observed during tests under larger stresses. During later tests performed on argillite samples, a different design was adopted (see Fig. 3): three samples were tested together, and six sensors were placed at the periphery of the circular plate. The results provided by the six sensors were quite consistent. In fact, the electronic part of the system was the weakest: its behaviour became non-linear under the severe hygrometric conditions experienced in the La Brasserie Quarry (see Section 2.5.2.).

### 2.3. Loading

In order to keep the applied stress as constant as possible, dead weights were used. Steel cylinders were set upon the upper silica plate lying on the upper face of the cylindrical sample. The applied stress is calculated by dividing the weight of steel cylinders set upon the upper plate by the initial cross-sectional area of the sample. No attempt was made to account for the (small) diameter changes experienced during the test.

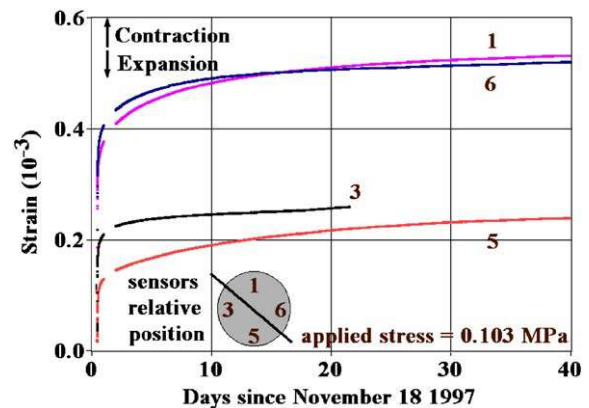


Fig. 4. Strain-versus-time curves measured at the beginning of Varangéville Test no. 1. Applied stress is 0.103 MPa.

### 2.4. Relative rotation of the two plates

Before the tests, displacements induced by temperature variations were measured thoroughly; they showed that the measurements provided by the four sensors were consistent. As soon as load was applied and, later, during the creep phase, the four sensor records begin to differ significantly, as shown by the four displacement-versus-time curves in Fig. 4 (Varangéville Test no. 1). This effect is mostly significant during the 10 first days. In fact, the average strain rates computed for each pair of sensors placed along the same diameter are close to one another. (The sum of the strains measured by sensors (1) and (5) approximately equals the sum of the strains measured by sensors (3) and (6), which strongly suggests that, rather than some erratic drift of the sensors, there is relative rotation of the two silica plates around a SE-NW horizontal axis; see Fig. 4). This rotation likely originates from geometrical defects of the sample faces. Special care was taken when planning each of the two sample faces (i.e., the defect height is smaller than  $2 \mu\text{m}$ ); however, the two faces are not perfectly parallel, and the sample height is non-uniform by several hundredths of a millimetre.

Non-uniform thermal loading generates similar phenomena. Light is provided by lamps that are switched on when one of the staff works in the mine gallery. Reversible rotations appear (The displacements measured by the four sensors are not equal.) as soon as the lamps are switched on; they are due to the uneven heating of the lateral surface of the samples by the lamps, which induces non-homogeneous thermal expansion.

### 2.5. Temperature and hygrometry

The temperature changes during a long-term creep test must be as small as possible and must be measured precisely enough to allow correction of the raw strain data for thermo-elastic strains. For these reasons, the tests were performed in deep underground openings, where temperature is much more constant than in any surface facility. Two sites were selected: Varangéville Mine and La Brasserie Quarry.

#### 2.5.1. Varangéville mine

With support provided by the Compagnie des Salins du Midi et Salines de l'Est, tests were performed on salt samples in a 700-m long, 160-m deep gallery of the Varangéville (France) salt mine. This gallery is remote from both the area of present salt extraction and the ventilation system. Fig. 5 displays temperature and hygrometry changes, continuously monitored from November 1997 to October 1998. (In the following, November 18, 1997 is the start date (day 1) and 0h00 on November 18, 1997 is the origin of time.)

Temperature, as are all other measured quantities, is recorded every 2min during the test. The average temperature is 13.5°C. Daily temperature variations, which are recorded with a resolution of one-thousandth of a degree Celsius, appeared to be of the order of  $\pm 0.01$ °C. These daily variations clearly correlate to variations of the ground diurnal temperature. Seasonal variations of a few hundredths of a degree Celsius also can be observed. In fact, the presence of humans in the

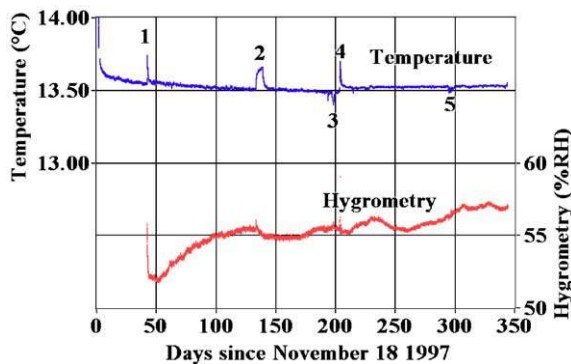


Fig. 5. Varangéville Mine: ambient temperature and hygrometry from November 18, 1997 (day 1) to October 26, 1998 (day 343).

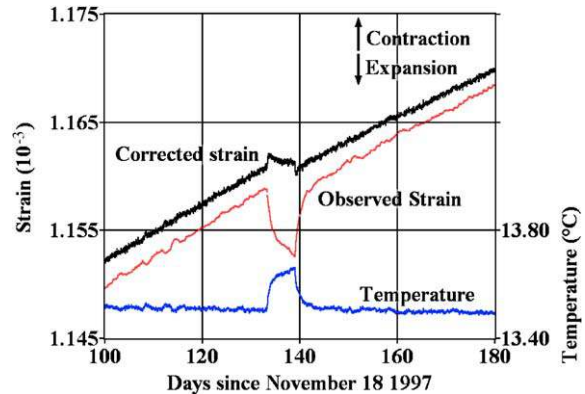


Fig. 6. As-observed axial strain and temperature variations during days 100–180, Varangéville Test no. 1, together with the strain variations corrected for temperature variations. An arbitrary strain offset of  $2.5 \times 10^{-6}$  was applied to the “corrected strain-versus-time” curve to make the figure easier to read.

gallery and power cuts that switch off electronic and software devices create the largest thermal perturbations. For example, temperature variations can be observed on Fig. 5 (The numbers between brackets refer to Fig. 5); these occurred during scheduled operations on days 42 (1) and 203–204 (4) and, resulting from unexpected power cuts, on days 193 (3) and 297 (5). On day 133 (2), a lamp was turned on and mistakenly remained on until the lamp burned out (about 6 days later) (see also Fig. 6 and Section 2.6). Depending upon the intensity and duration of the thermal perturbation, the return to thermal equilibrium took a few hours to several days.

During the same time period, hygrometry slowly increased from 52 to 57% RH and exhibited small, long-period fluctuations. Whether these changes are actual or due to hygrometry sensor drift is difficult to assess. (Hygrometry sensor precision is not better than  $\pm 2\%$ .)

#### 2.5.2. La Brasserie Quarry

With the assistance of the Inspection Générale des Carrières de Paris, tests were performed on argillite samples set in a 25-m deep room-and-pillar Quarry located in the Paris suburb of Vincennes. Measurements proved that daily temperature variations were smaller than a few hundredths of a degree Celsius. However, hygrometry in this Quarry is quite high (close to 100% RH), as the lake of the Vincennes Zoo is very close to the Quarry: a small amount of water continually permeates through the gallery roof. Although several steps were taken before the test to reduce sample desaturation during sampling, cutting and storage operations, and during the tests to insulate the samples, which were loaded to 1–3 MPa, re-saturation and swelling took place. Creep and swelling interfered, and clear distinction of each mechanism was difficult [12]. In

retrospect, testing argillitic rocks in such an environment was a mistake.

### 2.6. Correction for temperature variations

Temperature variations generate thermo-elastic strains. A striking correlation between temperature and strain variations can be observed on Fig. 6, which shows clear evidence of the thermo-elastic behaviour of rock salt. The empirical correlation coefficient is quite close to the thermal-expansion coefficient of the rock ( $\alpha = 4.4 \times 10^{-5} \text{ }^\circ\text{C}^{-1}$ )—indirect proof of the small influence of temperature on the silica sensor length. When corrected for temperature variations, the strain-versus-time curve is much smoother (see Fig. 6), although a few discontinuities remain; for example, during the time a lamp inadvertently remained on (day 133), the temperature was significantly higher (by  $0.15 \text{ }^\circ\text{C}$ ), leading to some creep acceleration. However, this acceleration probably was small. Usually, it is accepted that strain rate is proportional to  $\dot{\epsilon} \sim \exp(-Q/RT)$ , where  $T$  is the (absolute) temperature, and  $Q/R$  is a constant typically belonging to the range 4000–10000 K (see [13]). It follows that a  $dT$  temperature increase generates a relative increase in strain rate such that

$$d\dot{\epsilon}/\dot{\epsilon} = Q dT/RT^2$$

or, if we accept  $Q/R = 4100 \text{ K}$ ,  $d\dot{\epsilon}/\dot{\epsilon} = 7.5 \times 10^{-3}$  when  $dT = 0.15 \text{ K}$  and  $T = 286.5 \text{ K}$ .

Surprisingly, however, during this incident (days 133–139), the overall strain, when corrected for thermo-elastic variations, is smaller at the end of the heating period than it should have been had the temperature been kept constant. One possible explanation for this paradoxical result can be found in a concomitant hygrometry decrease.

### 2.7. Correction for hygrometry variations

Hunsche and Schulze [10] suggest that, when uniaxial creep tests are considered, the effect of humidity be taken into account by multiplying the “standard” steady-state creep rate ( $\dot{\epsilon}_{s0}$ ) by a factor  $\dot{\epsilon}_s = \dot{\epsilon}_{s0}(1 + w \sinh(q\Phi))$ , where  $\Phi$  is the relative air

humidity in % RH, and  $w$  and  $q$  are two constants. During our tests,  $\Phi$  varies in the range  $\Phi = 55 \pm 2$  (% RH). If we set  $\Phi_0 = 55\%$  RH, we get

$$d\dot{\epsilon}/\dot{\epsilon} = wq \cosh(q\Phi_0)d\Phi/(1 + w \sinh(q\Phi_0)).$$

Hunsche and Schultze suggest  $q = 0.1$  and  $w = 0.1$ . If these figures are accepted, a humidity change of 1% RH ( $d\Phi = 1$ ) leads to a relative change in creep rate:  $d\dot{\epsilon}/\dot{\epsilon} = 9 \times 10^{-2}$ . Although this change is significant, we did not try to correct observed displacements for hygrometry variations, as the exact accuracy and drift of hygrometry sensors are difficult to assess.

## 3. Creep under small load

Tests were performed in the Varangéville Mine on salt samples from the Etrez salt formation. Testing programme is given in Table 1. Earlier tests by Charpentier [14] and Pouya [15] have been performed under standard stress levels on samples from this formation.

### 3.1. Varangéville Test no. 1

On November 18, 1997 (day 1), Varangéville Test no. 1 started on a phenoblastic salt sample initially loaded to  $\sigma = 0.103 \text{ MPa}$ . The applied stress was modified twice: the initial applied stress was increased to  $\sigma = 0.108 \text{ MPa}$  (+5%) after day 42 (1) and then decreased to  $\sigma = 0.076 \text{ MPa}$  (−30%) after day 343 (4). Numbers between brackets refer to Fig. 7, which displays the strain-versus-time curve; this curve averages the data provided by the 4 displacement sensors. The strain rate ( $\dot{\epsilon}$ ) is computed every 5 days; it is averaged for a 10-day period. Strains are corrected for temperature variations; only the effect of a large temperature increase associated with the lamp incident (2), with the set-up (3) of Varangéville Test no. 2 on day 203 and with the end of Varangéville Tests no. 2 and 3 (5), remain visible. Strain experienced a long initial transient period up to day 150, at which time the average strain rate stabilized to  $\dot{\epsilon} = 1.4 \times 10^{-12} \text{ s}^{-1}$  (Sample contractions are positive.), with long-period amplitude fluctuations of  $\pm 20\%$ ; this

Table 1  
Testing programme

Day (since November 18, 1997)	1	42	204	343	520	660
Test no. 0 Duralumin sample	$\sigma = 0 \text{ MPa}$					
Test no. 1 Phenoblastic salt	$\sigma = 0.103 \text{ MPa}$	$\sigma = 0.108 \text{ MPa}$		$\sigma = 0.076 \text{ MPa}$		
Test no. 2 Pure salt			$\sigma = 0.102 \text{ MPa}$			
Test no. 3 Intermediate quality				$\sigma = 0.021 \text{ MPa}$	$\sigma = 0.054 \text{ MPa}$	

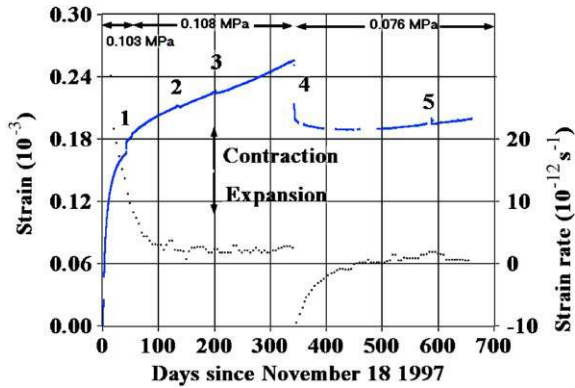


Fig. 7. Strain-versus-time and strain rate-versus-time during Varangéville Test no. 1.

possibly is related to fluctuations in hygrometry (see Section 2.5.1).

The 30% unloading performed on day 343 led to rapid axial expansion followed by a long period of time during which delayed axial expansion takes place. (Sample expansions are negative.) This delayed expansion can be observed up to day 450. During this period, recording was interrupted frequently due to failures of the measurement system. The transient inverse creep has been observed by several authors (e.g., [16,8]) and is sometimes referred to as a consequence of a “stress drop”. During this test, this inverse creep lasted much longer (100 days) than currently observed for tests involving larger stresses. Strain rate more-or-less stabilized after day 620, and  $\dot{\epsilon} = 7 \times 10^{-13} \text{ s}^{-1}$ .

### 3.2. Varangéville Test no. 2

On June 8, 1998 (day 203—i.e., 203 days after the earlier tests began), an identical creep apparatus was set on the same table, and, on day 204, Varangéville Test no. 2 started on a salt sample significantly purer than the former, loaded to a stress of  $\sigma = 0.102 \text{ MPa}$ . (Fig. 8; strains not corrected for thermoelastic variations). In this test, creep was faster than during Varangéville Test no. 1: from day 100 to 133 after the beginning of each test, the cumulated strain was  $2.5 \mu\text{m}$  for Varangéville Test no. 2 (“pure” salt) and  $1.8 \mu\text{m}$  for Varangéville Test no. 1 (“phenoblastic” salt). This difference is quite consistent with what is known from previous tests performed at larger stresses on these two salt types [15]. An increase in the strain rate, followed by an equivalent decrease, can be observed at day 343 (on which staff members were present in the gallery) and around day 500 (the strain rate evolutions were more progressive in this case). There is no definite explanation for these strain-rate changes. At the test’s end, the observed strain rate is  $\dot{\epsilon} = 1.8 \times 10^{-12} \text{ s}^{-1}$ .

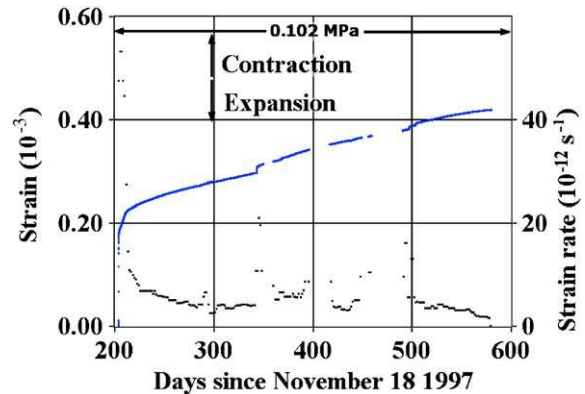


Fig. 8. Strain-versus-time and strain rate-versus-time during Varangéville Test no. 2.

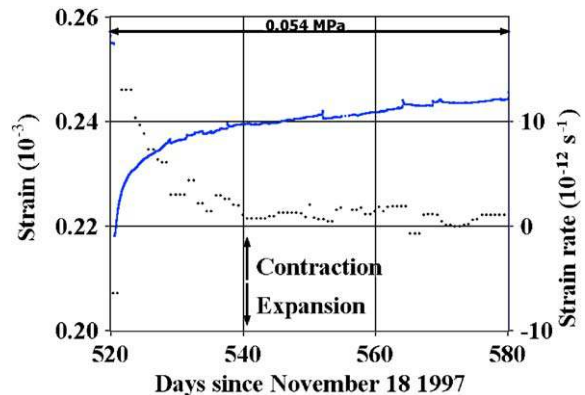


Fig. 9. Strain-versus-time and strain rate-versus-time during Varangéville Test no. 3.

### 3.3. Varangéville Tests no. 0 and 3

On November 18, 1997 (day 1), the reference test described in Section 2.2.1 (Varangéville Test no. 0) began on a cylindrical duralumin sample with geometrical dimensions similar to those used in Varangéville Test no. 1. No loading was applied on this sample. On October 26, 1998 (day 343), a third salt sample, of intermediate quality between pure and phenoblastic, was substituted for the reference sample when it appeared that reference test results probably were impaired by the existence of glue dots left at the bottom of the sample. This third sample was loaded to a stress of  $\sigma = 0.021 \text{ MPa}$  (Varangéville Test no. 3). No creep was observed even 177 days after the test began. The load probably was too small to generate any detectable strain. Then, the uniaxial load was built up to  $0.054 \text{ MPa}$  (+150%) by day 520. Creep is quite small (Fig. 9) but measurable. A long transient period can be observed, during which creep rate progressively decreases to  $\dot{\epsilon} = 1.2 \times 10^{-12} \text{ s}^{-1}$ . Large fluctuations in strain rate can be observed. Only one sensor is responsible for the small discontinuities observed on

the strain-versus-time curve (which averages the data provided by the four sensors).

#### 4. Comparison with tests performed under larger stresses

Qualitatively, the behaviour of salt under small stress ( $\sigma \approx 0.1$  MPa) exhibits the same general features as observed under larger stresses (say,  $\sigma = 5\text{--}20$  MPa). Rapid stress build-up leads to transient creep characterized by slow rate decrease. Creep rate then becomes roughly constant (steady state is reached) or, more precisely, its average value remains constant, but the rate experiences long-period fluctuations possibly influenced by slow changes in hygrometry. Loading decrease (“stress drop”) generates inverse creep, which lasts much longer than during tests performed under larger compressive stresses.

The Norton–Hoff constitutive law often is proposed to describe steady-state creep. Its uniaxial expression is

$$\dot{\epsilon} = A^* \exp(-Q/RT) \sigma^n,$$

where  $\sigma$  is the applied deviatoric stress,  $T$  is the absolute temperature, and  $A^*$ ,  $n$  and  $Q/R$  are constants. For Etrez salt, Pouya [15] suggests the following parameter values:

$$A^* = 0.64 \text{ MPa}^{-n} \text{ yr}^{-1}, \quad Q/R = 4100 \text{ K}, \quad \text{and} \\ n = 3.1.$$

If the Norton–Hoff law is extrapolated to conditions in Varangéville Test no. 1 ( $\sigma = 0.108$  MPa,  $T = 286.5$  K), the calculated strain rate (or  $\dot{\epsilon} = 10^{-17} \text{ s}^{-1}$ ) is smaller by 5 orders of magnitude than the observed strain rate ( $\dot{\epsilon} = 1.4 \times 10^{-12} \text{ s}^{-1}$ ). In other words, the observed strain rates, even if exceedingly small, are much larger than expected. Spiers et al. [17] suggest that pressure-solution (rather than dislocation climb and glide, which are the governing mechanisms for higher stresses) is the most effective creep mechanism when very small stresses are involved; the stress exponent in this context would be  $n = 1$  rather than  $n = 3\text{--}5$ , which is observed during standard tests. If this suggestion is adopted, the creep law must be modified when small stresses are considered, with significant consequences in the prediction of cavern or gallery convergence rate. It is interesting to note that the measured strain rate is consistent with estimations of the Newtonian viscosity of salt ( $\dot{\epsilon} = A \sigma$ ;  $\eta = 1/A = 10^{17}$  Pa s), which can be back-calculated from geological observations—e.g., the kinetics of salt dome rise [18].

#### 5. General conclusions

Long-term uniaxial creep tests were performed on rock salt samples (for 650 days) and argillite samples

(for 150–200 days—not fully described in this note). The applied loads were small ( $\sigma = 0.02\text{--}3$  MPa). Strain rates as slow as  $7 \times 10^{-13} \text{ s}^{-1}$  ( $2 \times 10^{-5} \text{ yr}^{-1}$ ) were observed in some cases. Such small loads and strain rates raise several specific problems: possible drift of the sensors during the 2-yr long tests, interference with small changes in room temperature and hygrometry, and effects related to non-uniform distribution of the load applied on sample surfaces. These difficulties have been recognized and at least partly addressed.

For Etrez rock salt, the qualitative results are in good agreement with what is known of rock salt behaviour under larger stresses; however, the observed strain rates, even if exceedingly small, were much larger than expected. Many lessons were learned during the course of testing under these unusually low stresses. These first series of tests opened the way for further investigation of rock behaviour under very small stresses, an important issue both for geological and engineering applications.

#### Acknowledgements

The authors are indebted to Compagnie des Salins du Midi et Salines de l’Est and to Inspection Générale des Carrières de Paris, whose kind help has been instrumental. The tests on argillite were sponsored by ANDRA, the French Agency in charge of radioactive-waste disposal and by the CNRS (the French National Research Agency) through the GdR FORPRO (Research action number 2000.I), and part of this work corresponds to the GDR FORPRO contribution number 2003/21 A. The authors also are indebted to J. Lancelot, Head of the FORPRO programme. The authors benefited from comments by J.P. Gratier. Special thanks to K. Sikora.

#### References

- [1] Brouard B. On the behaviour of solution-mined caverns. PhD thesis, Ecole Polytechnique, France, 1988 [in French].
- [2] Bérest P, Bergues J, Brouard B, Durup JG, Guerber B. A salt-cavern abandonment test. *Int J Rock Mech Min Sci* 2001;38(2): 343–55.
- [3] Hardy Jr RH, Langer M, editors. Proceedings of first conference on the mechanical behavior of salt. Clausthal-Zellerfeld, Germany: Transactions of Technical Publishers; 1984 901p.
- [4] Hardy Jr RH, Langer M, editors. Proceedings of second conference on the mechanical behavior of salt. Clausthal-Zellerfeld, Germany: Transactions of Technical Publishers; 1988 781p.
- [5] Hardy Jr RH, Langer M, Bérest P, Ghoreychi M, editors. Proceedings of third conference on the mechanical behavior of salt. Clausthal-Zellerfeld, Germany: Transactions of Technical Publishers; 1996 621p.
- [6] Aubertin M, Hardy Jr RH, editors. Proceedings of fourth conference on the mechanical behavior of salt. Clausthal-



- Zellerfeld, Germany: Transactions of Technical Publishers; 1998 658p.
- [7] Cristescu N, Hardy Jr RH, Simionescu RO, editors. Proceedings fifth conference on the mechanical behavior of salt. Lisse: Swets & Zeitlinger; 2002 466p.
- [8] Hunsche U. Measurement of creep in rock salt at small strain rates. In: Proceedings of second conference on the mechanical behavior of salt. Clausthal-Zellerfeld, Germany: Transactions of Technical Publishers; 1988. p. 187–96.
- [9] Horseman ST. Moisture content—a major uncertainty in storage cavity closure prediction. In: Proceedings of second conference on the mechanical behavior of salt. Clausthal-Zellerfeld, Germany: Transactions of Technical Publishers; 1988. p. 53–68.
- [10] Hunsche U, Schultze O. Humidity induced creep and its relation to the dilatancy boundary. In: Proceedings of fifth conference on the mechanical behavior of salt. Lisse: Swets & Zeitlinger; 2002. p. 73–88.
- [11] Bérest P, Charpentier JP, Blum PA. Creep of rock under small loading. In: Proceedings of SMRI fall meeting, Washington DC, 1999. p. 11–24, Proceedings of the “SMRI Meetings” are available at: SMRI-3336, Lone Hill Lane, Encinitas, CA 92024-7262, USA.
- [12] Charpentier JP, Gharbi H, Valès F, Bérest P, Blum PA. Creep of argillites under small mechanical loading. In: Delage P, editor. Proceedings of the sixth international workshop on key issues in waste isolation research (ENPC, Paris), 2001. p. 199–214.
- [13] Brouard B, Bérest P. A classification of salt according to their creep properties. Proceedings of SMRI spring meeting, New Orleans, 1998. p. 18–38.
- [14] Charpentier JP. Creep of rock salt at elevated temperature. In: Proceedings of second conference on the mechanical behavior of salt. Clausthal-Zellerfeld, Germany: Transactions of Technical Publishers; 1988. p. 131–6.
- [15] Pouya A. Correlation between mechanical behavior and petrological properties of rock salt. In: Roegiers JC, editor. Proceedings of 32nd US symposium on rock mechanics. Rotterdam: Balkema; 1991. p. 385–92.
- [16] Munson D, Dawson P. A transient model for salt during stress loading and unloading. Albuquerque, NM: SAD 82-0962, Sandia National Laboratories; 1982 55p.
- [17] Spiers CJ, Urai JL, Lister GS. The effect of brine (inherent or added) on rheology and deformation mechanisms in salt-rock. In: Proceedings of second conference on the mechanical behavior of salt. Clausthal-Zellerfeld, Germany: Transactions of Technical Publishers; 1988. p. 89–102.
- [18] Odé H. Review of mechanical properties of salt relating to salt dome genesis. In: Saline deposits-geological society of America, Special Paper 88, 1968. p. 543–95.